Intercalation Kinetics of Long Polymers in 2 nm Confinements

E. Manias,[*,‡] **H. Chen,**[†] **R. Krishnamoorti,**[§] **J. Genzer,**[⊥] **E. J. Kramer,**[#] **and E. P. Giannelis**[†]

*Department of Materials Science & Engineering, Cornell University, Bard Hall,
Ithaca, New York 14853-1501; Department of Materials Science & Engineering,
The Pennsylvania State University, 310 Steidle Building, University Park, Pennsylvania 16802;
Department of Chemical Engineering, University of Houston, Houston, Texas 77204; Department of
Chemical Engineering, North Carolina State University, Raleigh, North Carolina 27695; and
Materials Department and Department of Chemical Engineering, University of California at
Santa Barbara, Engineering III, Santa Barbara, California 93106*

Received May 31, 2000; Revised Manuscript Received August 21, 2000

ABSTRACT: The motion of confined polymers is measured experimentally between parallel, atomically smooth solid surfaces, separated by 2 nm. In particular, the kinetics of intercalation of monodispersed polystyrene in alkylammonium modified mica-type silicates were studied using X-ray diffraction. The kinetics of the neat polymers and their functionalized derivatives were measured as functions of molecular weight, extent of functionalization, and silicate surface organic modification, at various temperatures. Selective corroborative studies were also performed using in-situ small-angle neutron scattering (SANS). The kinetic data are interpreted in terms of an effective diffusion coefficient (D_{eff}) of the polymer, which undergoes a dramatic decrease with stronger silicate surface−polymer interaction. This interaction is varied by either changing the silicate surface modification or by increasing the extent of functionalization of the polystyrene chains. Furthermore, the diffusion coefficient exhibits an inverse dependence on chain length (N), i.e., $D_{eff} \propto N^{-1}$, for chains up to 900 000 molecular weight.

I. Introduction

The dynamics of polymers confined in spaces smaller or comparable to their dimensions are dramatically different than in the equivalent bulk,[1−11] not only because the chain conformations are substantially deformed due to geometric constraints but also because the polymers are affected by the surface−polymer interactions.[1,2] Recent molecular dynamics (MD) simulation studies have revealed that the dynamics of the chain molecules undergo radical changes in the vicinity of solid surfaces. Namely, both the chain mobility[1] and the chain relaxation times[2] can be slowed by 3 orders of magnitude near physisorbing surfaces. Moreover, extensive surface forces apparatus (SFA) experiments report how these novel dynamics of nanoconfined polymers are manifested through viscosity increases, to values orders of magnitude higher than the bulk values, solidlike responses to imposed shear, and confinement induced "sluggish" dynamics that suggest the existence of a "pinned", "immobilized" layer adjacent to the confining mica surfaces.[3−10] In this work we explore experimentally the mobility of polymers in the immediate vicinity of surfaces, and specifically their motion when confined between atomically smooth, crystalline, mica-type silicate layers separated by 20 Å.

Increased interest has been recently concentrated on polymer intercalated into 2:1 mica-type phyllosilicates, such as montmorillonite and synthetic hectorites, as model systems for studying the structure and dynamics of nanoscopically confined polymers.[12,13] Intercalation of a wide variety of polymers into the silicate galleries is accomplished, after rendering hydrophobic—the normally hydrophilic inorganic host surface—through ion exchanging the hydrated inorganic gallery cations (Na^+, Li^+, Ca^{2+}) with cationic organic surfactants, such as alkylammoniums. In many cases, polymer melts can intercalate directly, *unassisted by shear or solvents*.[14] This fact is rather surprising as it implies that polymer chains can undergo large center-of-mass displacement (up to several micrometers) in almost two-dimensional interstices. Pioneering studies by Vaia et al.[15] utilized a simple XRD-based scheme to investigate the kinetics of polystyrene (PS) intercalation in octadecylammonium exchanged fluorohectorite (C18FH) under quiescent conditions.

In the present work, we expand upon these previous studies[15] and present a systematic study of the kinetics of polymers entering 2 nm wide galleries of mica-type silicates as a function of polymer M_w and polymer−surface interactions. We vary the polymer−surface energetics in two ways: either through changing the surface modification (by varying the organic coverage) or through attaching strongly interacting sites—sticky groups—along the polymer chain.

II. Systems, Materials, and Methods

Background. The systems studied in this work are polymers intercalated—inserted—in a synthetic 2:1 layered silicate. A representation of the experimental system is shown in Figure 1. These systems have many advantages for the study of the polymer mobility in the *immediate vicinity* of a surface. The confining geometries are extremely well defined, since the polymer is intercalated between the cleavage planes of mica-type layered inorganic hosts with atomically smooth surfaces, typical lateral dimensions of ∼5 μm, and when intercalated assemble parallel to each other separated by a
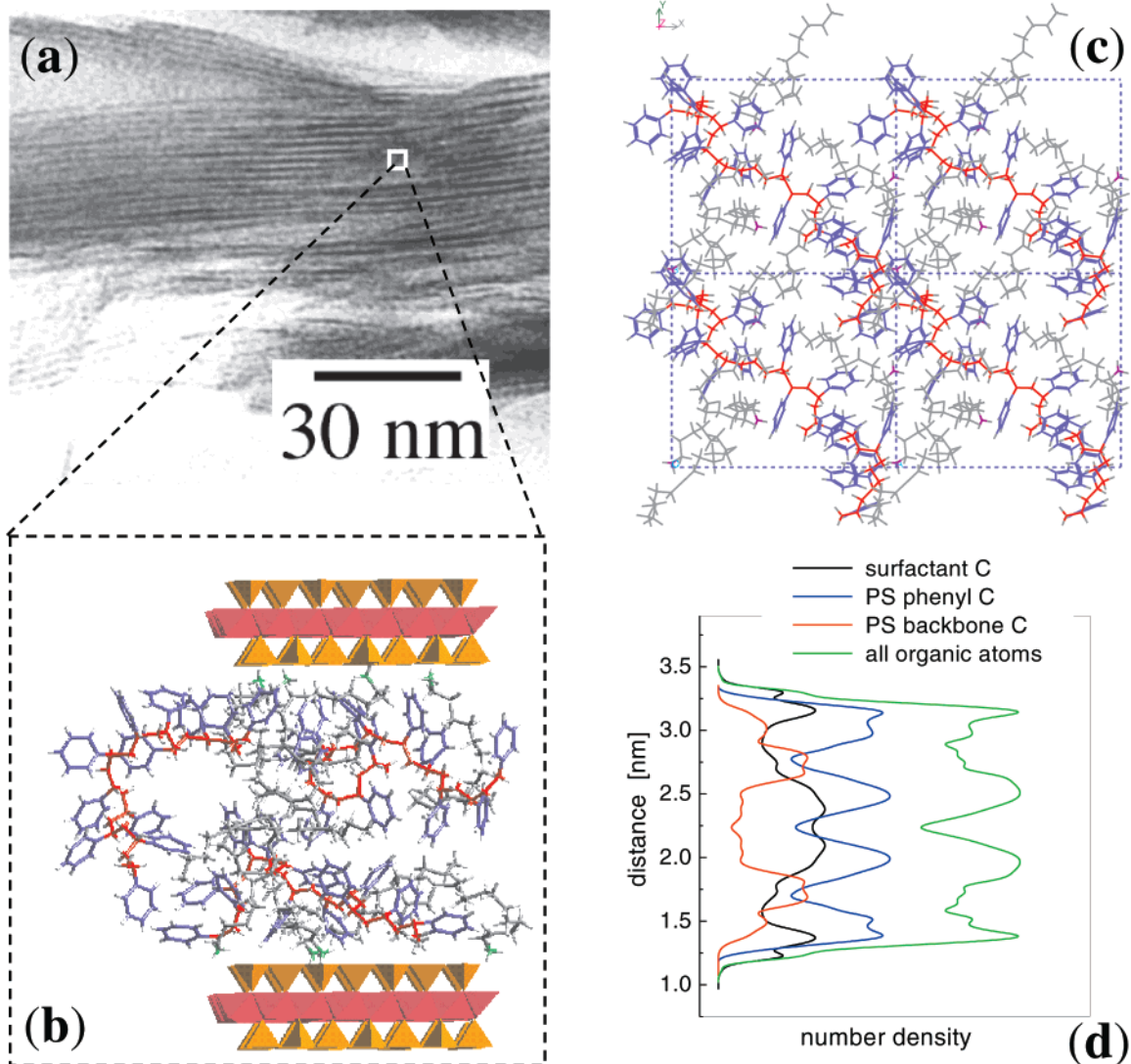
[†] Cornell University.
[‡] The Pennsylvania State University.
[§] University of Houston.
[⊥] North Carolina State University.
[#] University of California at Santa Barbara.
[*] Address correspondence to: manias@psu.edu or epg2@cornell.edu.

Figure 1. Some representations of the experimental system geometry: (a) a TEM bright field image showing an alternating silicate (dark) and polymer (gray) layers; (b, c, d) snapshots from computer modeling studies; (b) a cross section of the confined film, (c) a typical configuration parallel to the confining surfaces (for clarity the lower half of the film from four simulation boxes is shown); and (d) the density profiles of the different carbon atoms across the intercalated film. The same colors are used for the PS backbone, PS phenyl, and surfactant in (b) and (c), as well as for their respective density profiles in (d). The width of the inorganic layers is 9.7 Å, whereas the width of the confined organic film is 20 ± 1 Å.

well-defined distance of 20 ± 1 Å. This ordering is very strong and gives rise to intense wide-angle X-ray diffraction peaks with up to 11 orders of reflections— for the PS/FH systems studied here.

During the insertion of the polymer in these nanometer galleries, the effective diffusion constants are several orders of magnitude higher than the polymer diffusion[15] in the presence of all the intercalated chains. Although this means that we study a motion that does not correspond to the "tracer diffusion" of the confined polymer, at the same time this mobility enhancement makes these experiments possible since we can observe molecular motion in time scales of a few hours at temperatures less than 100 °C above the bulk T_g. We expect that the same mechanisms that determine the intercalation kinetics will also govern the self-diffusion of a physisorbed polymer chain at equilibrium with other identical polymers next to a confining surface.[16,17] This expectation is also supported by recent computer simulation studies which show that the assumptions of the Fickian diffusion theory are still valid where motion takes place under strong chemical potential gradients[18]

and for polymers intercalating into the galleries of layered silicates.[19]

The wide-angle X-ray diffraction (XRD) method[15,20] that we employ has two main advantages. First, by following the evolution of a specific reflection in the XRD pattern, we can discriminate and follow only the motion of those polymers between parallel surfaces separated by a well-defined distance. In our case, the d_{001} diffraction peak corresponds to $d \simeq 30$ Å, which means that we study the motion of polymers between parallel mica-type layers separated by approximately 20 Å.[21] Moreover, in this method the ratio of the integrated intercalated intensity is measured with time and normalized by the diffracted intensity of a reference material introduced in our samples; in this way there is only one fitting parameter—the effective diffusion constant—for the whole annealing time series.[15] Finally, where the silicate size is known, this method has been successful in determining quantitatively the diffusion constants for the intercalation of both small molecules,[20] as well as long polymer chains[15] intercalated in layered silicates. More details regarding the data collection and analysis

Table 1. Weight-Average Molecular Weights, Polydispersity Indices, and Bromine Content for the Various Styrene Polymers Used in the Current Study[a]

polymer	M_w	M_w/M_n	polymer	PS M_w	x (% Br)
PS	35 000	1.06	PBr$_x$S	90 000	3.8
PS	50 000	1.06	PBr$_x$S	90 000	8.7
PS	65 000	1.04	PBr$_x$S	90 000	15.2
PS	90 000	1.04			
PS	152 000	1.05	PBr$_x$S	152 000	2.8
PS	200 000	1.05	PBr$_x$S	152 000	7.9
PS	400 000	1.06	PBr$_x$S	152 000	15.1
PS	575 000	1.06			
PS	900 000	1.07	PBr$_x$S	575 000	3.3
PS	1 880 000	1.30	PBr$_x$S	575 000	9.2

[a] The bromination level reported is an average bromine percentage per chain as measured by elemental analysis.

can be found in other studies.[15,22] The widths of the original unintercalated peak and the final intercalated peak appear to be similar, suggesting that the polystyrene melt intercalation does not alter markedly the coherence length, or disrupt the layer structure, of the silicate crystallites. In addition, post-intercalation TEM studies of the polymer/organosilicate hybrids used in this study never revealed any exfoliated or disordered silicate layers, as have been reported before for perbrominated PS in C12FH.[23]

Theoretical derivations and MD computer simulations[19] of the motion of polymers in slit pores confirm that the time evolution of the intercalated diffracted intensity $I(t)$ and the effective polymer diffusional time τ_{diff} within the slit are related by eq 1, which we use to fit the experimental data:

$$\chi(t) \equiv \frac{I(t)}{I(\infty)} = 1 - \sum_{m=1}^{\infty} \frac{4}{a_m^2} \exp\left(-\frac{a_m^2\, t}{\tau_{eff}}\right) \qquad (1)$$

where τ_{diff} is the effective diffusional time constant, for which $1/\tau_{diff} \equiv D_{eff}/a^2$, with D_{eff} an effective diffusion coefficient and a the mean silicate size; and a_m are the roots of the zeroth-order Bessel function ($J_0(x) = 0$). The fraction of intercalated polymer is given by the corresponding fraction of the XRD integrated intensities $\chi(t) = I(t)/I(\infty)$. The only adjustable parameter is τ_{diff}, which is estimated by fitting eq 1 to the XRD time series, and can be subsequently converted to the effective polymer diffusion coefficient (D_{eff}) by measuring the mean silicate size a. For our systems a can be directly measured by TEM and is approximately 5 μm.[15] Equation 1 was initially derived and extensively used for the intercalation kinetics of small molecules—such as solvents[20]—but has been recently applied to the problem of polymer intercalation in both experimental studies[15] and computer simulation approaches.[19]

Experiment. We selected to use model materials: Polystyrene, which is the polymer used throughout this study, can be obtained in a wide range of molecular weights with very good monodispersities, and its mobility has been studied extensively in the bulk,[24,25] at interfaces,[26] and in confined geometries,[27,28] as well as in mutual diffusion with other polymers.[29] All neat PS polymers were purchased from Pressure Chemicals, and their characteristics are summarized in Table 1. The layered host that we selected was fluorohectorite (FH), a synthetic 2:1 silicate, whose characteristics are much better defined than any naturally occurring silicate. Its lateral layer dimensions have a much narrower distri-

bution than the naturally occurring silicates, and its cation exchange capacity (which determines the surfactant grafting density[13]) is 1.50 mequiv/gr, which corresponds to a grafting density of 1 surfactant molecule per 87 Å^2. This grafting density is a mean value, based on the fact that there is exactly one surfactant molecule per isomorphous substitution in the synthetic FH. The exchange capacity of the silicate layers denotes the number of isomorphous substitutions, and TGA measurements (especially for a series of surfactants with different molecular weights as here) provide a very accurate method to obtain the CEC and hence the surfactant grafting density. As would be expected, even for these synthetic layered materials, there may be some heterogeneity between layers and within a layer, but this would be much smaller than the naturally occurring equivalents (montmorillonites or hectorites). Our TGA studies for dodecyl- through octadecyl-modified FH give a value of 87 Å^2/surfactant, which is in agreement with previous work.[45] The larger size layers were isolated by fractionating centrifugation and were subsequently exchanged by alkylammonium cationic surfactants (Aldrich) following the same procedure as before.[15]

While Vaia et al.[15] made XRD measurements on similar systems during in-situ annealing, we have made several enhancements that enabled us to study the kinetics ex-situ, i.e., by sequential annealings in a vacuum oven and subsequent XRD studies. The ex-situ method has several advantages over the in-situ method: First, we are able to anneal under vacuum, thus reducing any polymer decomposition. Postkinetics GPC examination of the polymer samples studied revealed no polymer decomposition for all the systems reported herein, even for the highest of temperatures used. Second, we can heat and subsequently investigate by XRD the same side/surface of the pellet sample, a procedure that provides a much more accurate control of the annealing temperature than in the in-situ case, where the pellet is heated from the one side and is studied by XRD on the opposite side. Moreover, we simultaneously anneal several samples in the same setup and under identical conditions, and thus we have more accurate comparison when changing an experimental parameter, e.g., annealing several samples of varying M_w under the exact same temperature and vacuum conditions. Furthermore, we mark the pellet so that we can always scan the same region of the sample in sequential X-ray runs, and by normalizing with the diffracted intensity of a reference material incorporated in each sample, we can superimpose the data for different annealing times, since we can normalize out the instrumental/sample deviations between different scans. Minute amounts of soapstone in each sample were used as a reference material, because it has a strong XRD reflection at 9.7 Å and does not undergo any phase transitions in the temperature range that we study, while at the same time it is stable in the presence of polymers.

The polymer−surface affinity is varied, because it is suggested[1] to be the most crucial parameter, since it controls the polymer−surface monomeric friction coefficient[30] and thus determines the motion of the polymer next to a solid surface. The energetics between the polymer and the surface are varied in two distinct, well-controlled ways: (i) keeping the polymer the same and modifying the surface, via controlled surface covering

by surfactants of varying length at the same grafting density, and (ii) keeping the organically modified surface the same and modifying the polymer friction coefficient, by attaching along the polymer chain a controlled amount of groups that interact strongly with the silicate surface.

Several comparative studies by concurrent in-situ small-angle neutron scattering (SANS) and intermediate-angle neutron scattering (IANS) were performed on NG3 at the Cold Neutron Research Facility at NIST, Gaithersburg, MD. Neutrons with wavelengths (λ) of 6 or 9 Å with $\Delta\lambda = 0.15$ Å were used with sample-to-detector distances ranging from 1.3 to 13.17 m. SANS measurements were performed to monitor the changes in dimensions of the polymer, i.e. R_g, and also to follow the changes in the single chain scattering function during intercalation. The details of these experiments are provided in a separate publication[31] and involved using isotopic blends of polystyrene and organically modified silicates. The intercalation kinetics were examined by neutron scattering at 160 °C.

Finally, to obtain some insight into the atomistic details of the structure of the confined—intercalated—polystyrene chains, we have also carried out molecular simulations. As details of the simulations are given elsewhere,[32] here we make only brief mention of the techniques employed. The rotational-isomeric-state (RIS) model was used to create initial polymer conformations of PS oligomers.[33] Conformations that fit in the interlayer gallery were chosen, and the PS chains were equilibrated by an off-lattice Monte Carlo scheme that employed small random displacements of the backbone atoms and orientational biased Monte Carlo rotations of the phenyl rings; at the same time, the surfactants were equilibrated by a configurational biased Monte Carlo (CBMC) scheme in coexistence with the polymer chains. After equilibration, molecular dynamics simulations were used to obtain the structure (Figure 1b) and density profiles (Figure 1d) of the intercalated polymer/surfactant films. The numbers of polymer chains and alkylammonium surfactants were chosen so as to match the densities found in the experimental studies (e.g., Table 4). While several force fields have been proposed for PS,[34] the force field of Müller-Plathe[35] was chosen, because when combined with the force field we have developed for the organosilicates,[36] it reproduces the experimentally observed d-spacings. While the full power of MD is most often used to probe dynamical properties—and such a study is currently underway—the limited time scales simulated to date in our MD studies can only provide accurately a detailed picture of the structure within the interlayer gallery.

III. Experimental Results and Discussion

Vaia et al.[15] studied the intercalation kinetics of PS in octadecylammonium exchanged fluorohectorite (C18FH) and found them to be of the same order of magnitude as transport by self-diffusion of polystyrene. These first results suggested that the process of intercalation was limited by the transport of polymer into the primary particles of the silicate and not specifically by transport of polymer chains inside the silicate galleries.[15] Expanding on these investigations, the work reported herein utilizes a range of polymers with much higher molecular weights (Table 1) and several layered hosts and shows that the interpretation of Vaia et al. does not always hold.
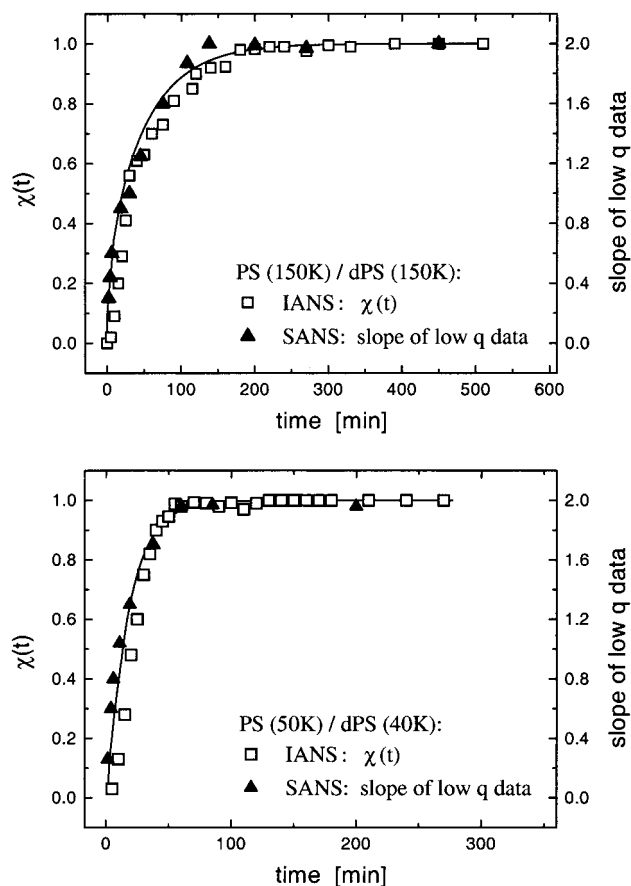
Figure 2. Concurrent small-angle neutron scattering (SANS) and intermediate-angle neutron scattering (IANS) measurement of the intercalation kinetics for two polystyrene isotopic blends; the lines are their common fits by eq 1. SANS monitors the conformational changes of the polymer chains as they enter the slit pore (through the slope of the low q data), and the concurrent IANS follows the slit pore expansion ($\chi(t)$), identically to the XRD studies. The excellent agreement of the two results is a proof that the gallery expansion is directly correlated to the polymer motion.

A. Small- and Intermediate-Angle Neutron Scattering. Concurrent in-situ small-angle neutron scattering (SANS) and intermediate-angle neutron scattering (IANS) were carried out to further validate the XRD method. The slope of the low-q SANS intensity changes from almost zero (i.e., independent of q) in the case of unintercalated samples to a final slope of $\sim q^{-2}$ when allowing sufficient annealing time for fully intercalated structures to be formed (Figure 2). These SANS measurements reflect the changing conformation of the PS molecules, clearly demonstrating the change from three-dimensional random walk statistics to a conformation consistent with the more restrictive intercalation geometry, that are suggested to be consistent with a directed two-dimensional random walk.[31] At the same time, concurrent in-situ intermediate-angle neutron scattering experiments were used to follow the intercalation kinetics by monitoring the gallery height. The change in the gallery spacing observed by IANS is analogous to the XRD measurements and reflects the overall registry of the silicate layers. Measurements carried out with pure protonated PS, perdeuterated PS, and isotopic blends all revealed the same overall trend, i.e., same silicate separation and registry, in very good quantitative agreement with the respective XRD studies. From Figure 2 it becomes obvious that there is a
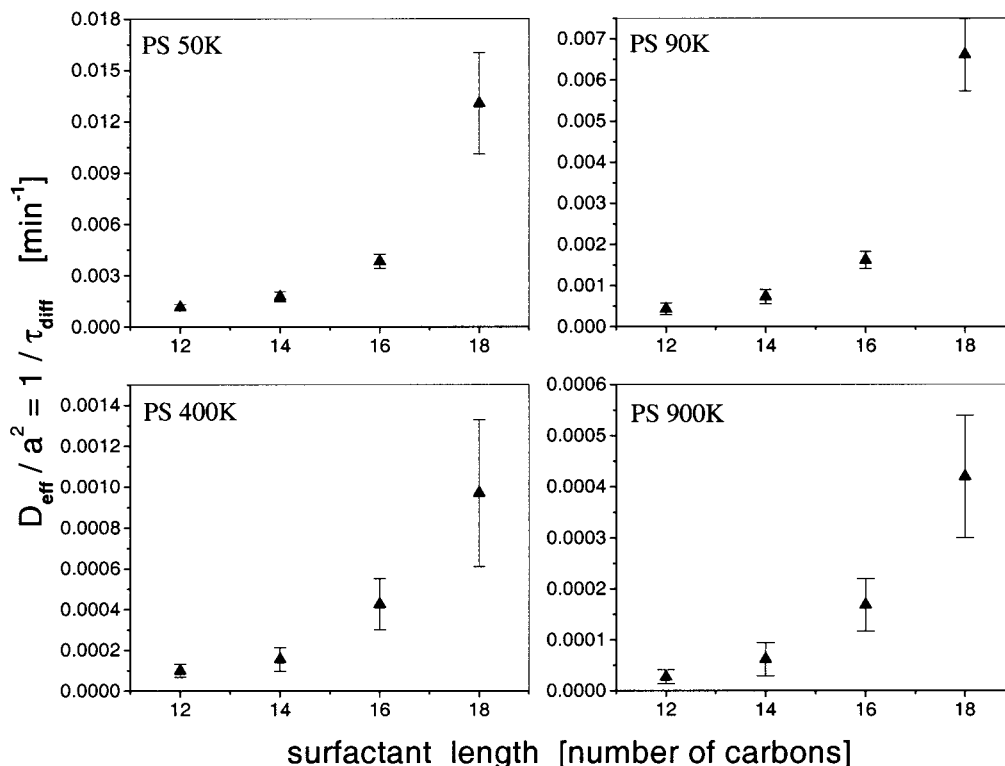
Figure 3. Diffusion coefficient versus the length of the alkyl chain of the surfactant; from the intercalation kinetics of PS in fluorohectorite at 170 °C for four different molecular weights (M_w: 50K, 90K, 400K, and 900K). The relative decrease of the diffusion times ($\tau_{eff} = a^2/D_{eff}$) from the dodecylammonium (C12) to octadecylammonium (C18) is typically from 10 to 15 times, and for the data shown $\tau_{eff}^{(12)}/\tau_{eff}^{(18)} \equiv D_{eff}^{(18)}/D_{eff}^{(12)} = 11.3$, 14.2, 9.7, and 14.5 times with ascending molecular weight.

direct correlation between the two measurements—chain conformations and silicate gallery spacing—and fittings to both sets of data with eq 1 yield the same values—within their uncertainty—for the polymer diffusion coefficient D_{eff} or time constant τ_{diff}.

B. Effect of the Polymer—Surface Interactions. Taking a clue from the findings of molecular simulations[1] and theoretical considerations, we first explore the effect of the polymer—surface interaction on the motion of the intercalating polymers. We employ two methods to change this interaction: (i) we modify the surface and intercalate the same polymer, and (ii) we keep the surface the same and intercalate polymers of varying adsorption energy for the surface.

(i) One general way to change the surface attraction, in experiments probing the motion of polymers near surfaces, is to graft small organic molecules on the confining surfaces. In previous studies by Leger and co-workers, octadecyltrichlorosilane (OTS) surfactants were used to cover a silica surface.[37] By decreasing the grafting density of the aliphatic surfactants, they could increase the surface area of silica exposed to the polymer and thus increase the polymer—surface interactions.[37] In our case, since the grafting density is constant and characteristic of the silicate, we can control the area of the silicate surface exposed to the polymer by varying the size of the surfactant while the grafting density remains the same (one surfactant per 87 Å^2 of silicate surface). This can be achieved by keeping the same chemical structure for the surfactant, namely alkylammonium, and varying the alkyl length, from dodecyl, to tetradecyl, to hexadecyl, and octadecylammonium (the respective organically modified silicates are denoted hereafter as C12FH, C14FH, C16FH, and C18FH). The

difference between the initial and final d spacings for each of the intercalated structures, i.e., the thickness of the organic interlayer, is the same for all the four systems with different surfactant lengths. Moreover, confinement induced changes in the polymer dynamics are not expected to differ substantially in systems where we vary the surfactant length from dodecyl- to octadecyl-ammonium.[59] In Figure 3 we show the typical dependence of the effective diffusion coefficient as a function of the surfactant length for various polymers. The polymer diffusion coefficient D_{eff} increases considerably with the length of the surfactant—typically 10-fold going from 12 to 18 carbons (Figure 3 and also Tables 3 and 4).

Finally, entropic effects associated with the different surfactant lengths[45,46] suggest that the intercalation kinetics should become faster for longer surfactants, in contrast with the experimental behavior. However, these entropic factors are calculated to be much smaller in magnitude than the associated enthalpic changes, due to the change of the exposed silicate area.[45]

(ii) A more straightforward approach—to establish the determining factor that controls the mobility of adsorbed polymer chains—is to retain the surface modification (use the same surfactant) and change the polymer affinity for the surface. This can be achieved by attaching along the polymer chain *sticky groups* that interact strongly with the silicate surface, which in fact consists of packed silicon oxide tetrahedra. A convenient way is to substitute the phenyl hydrogen in the para position by bromine for a small fraction of the monomers (3–15%). There are several advantages to this approach. Bromine is a group that interacts very strongly with silicon oxide surfaces.[38] Through a simple wet chemistry
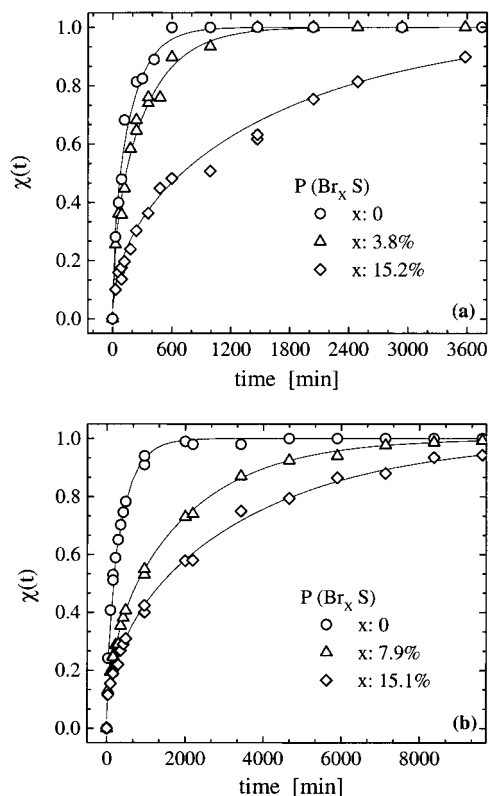
Figure 4. Representative raw data (symbols) and the fits by eq 1 (lines) of PS (a: $M_w = 90K$; b: $M_w = 152K$) and two of its brominated derivatives intercalated in $C_{14}FH$. The D_{eff} values from the fits shown, as well as for other systems, are tabulated in Table 2. Increasing the polymer–surface interactions—by adding more sticky Br groups across the polymer chain—results in substantial decreases of the polymer mobility in the confined film.

scheme one can brominate a controlled fraction of the para positions[39] of the phenyl groups along the polystyrene chain, and a series of monodispersed polymers can be created with varied levels of Br substitution (Table 1). Thus, the interaction energy per chain can be varied systematically, while retaining the same polymer molecular weight and polydispersity.

The introduction of such small amounts of Br does not alter markedly the bulk T_g of the polymer or its tracer diffusion in the bulk [Appendix B]. The glass transition temperature of the brominated polystyrenes from Table 1 ($x_{Br} < 15\%$) was measured with DSC and ranged from 101 to 103 °C, in good agreement with previously reported values.[40] At the same time such small bromination levels do not alter in any measurable extent the intercalated structure in the organosilicates used here; the XRD diffraction peaks appear at identical d spacings and have the same widths for all our brominated and neat polystyrenes in each organosilicate. Moreover, extensive post-intercalation TEM studies of the samples never showed any disordered silicates layers, like those observed in slightly disordered structures of perbrominated ($x_{Br} = 100\%$) polystyrenes into $C_{12}FH$.[23]

In Figure 4 we show two characteristic examples of the dependence of the polymer mobility on the substitution degree of the para hydrogens by Br. The fraction of the XRD integrated intensities $\chi(t)$ is shown for two PS ($M_w = 90\ 000$ and $152\ 000$) and two of their bromo-functionalized derivatives in $C_{14}FH$. The fitted values of corresponding effective diffusion coefficients are

Table 2. Inverse Diffusional Time Constants for Some of the Lightly Brominated Series of PBr$_x$S, at 170 °C[a]

PS M_w	x (%)	surface	D_{eff}/a^2 (min^{-1})
90K	0	$C_{16}FH$	$(1.58 \pm 0.12) \times 10^{-3}$
90K	3.8	$C_{16}FH$	$(1.50 \pm 0.07) \times 10^{-3}$
90K	8.7	$C_{16}FH$	$(1.41 \pm 0.07) \times 10^{-3}$
90K	15.2	$C_{16}FH$	$(0.54 \pm 0.03) \times 10^{-3}$
90K	0	$C_{14}FH$	$(8.21 \pm 0.60) \times 10^{-4}$
90K	3.8	$C_{14}FH$	$(4.70 \pm 0.19) \times 10^{-4}$
90K	8.7	$C_{14}FH$	$(1.80 \pm 0.14) \times 10^{-4}$
90K	15.2	$C_{14}FH$	$(0.88 \pm 0.07) \times 10^{-4}$
152K	0	$C_{14}FH$	$(4.18 \pm 0.97) \times 10^{-4}$
152K	2.8	$C_{14}FH$	$(3.13 \pm 0.75) \times 10^{-4}$
152K	7.9	$C_{14}FH$	$(0.82 \pm 0.08) \times 10^{-4}$
152K	15.1	$C_{14}FH$	$(0.45 \pm 0.07) \times 10^{-4}$
152K	0	$C_{12}FH$	$(28.40 \pm 1.85) \times 10^{-5}$
152K	2.8	$C_{12}FH$	$(2.78 \pm 0.58) \times 10^{-5}$
152K	7.9	$C_{12}FH$	$(0.50 \pm 0.12) \times 10^{-5}$
152K	15.1	$C_{12}FH$	$(0.19 \pm 0.05) \times 10^{-5}$

[a] The fitted value of $1/\tau_{diff} = D_{eff}/a^2$ from eq 1 is given. For longer polymers and/or higher bromination levels the diffusion coefficients are so small that they cannot be accurately evaluated even for the highest annealing temperatures employed: e.g. from the initial intercalation stages of a 25% brominated PS, the D_{eff} decreased more than 3 orders of magnitude compared to the neat PS in both C14FH and C12FH.

tabulated in Table 2 together with other systems, where we compare the D_{eff} of the neat polystyrenes with three bromination levels in three of the organically modified FHs. There is a systematic decrease of D_{eff} with higher bromination levels, and the decrease is much more dramatic for the surfaces bearing shorter surfactants, where more of the silicate surface is exposed to interact with the bromine groups. For surfaces bearing relatively long end-grafted surfactants (e.g., hexadecylammonium) C16FH the effect of increasing bromination degree is quite small. For example, bromination of 15% of the monomers results in a moderate, 3-fold only, decrease of the polymer D_{eff} compared to that of the unmodified PS, whereas for shorter surfactants, for example tetradecylammoniums, D_{eff} of similarly brominated polystyrenes ($x \simeq 15\%$) is reduced almost by 10 times compared to that of the respective unmodified PS ($x = 0$). With further decrease in the surfactant length, i.e., for a dodecyl-modified surface, the D_{eff} of the 15% brominated PS becomes 150 times smaller than the D_{eff} of the unmodified polymer for the same surfaces (Table 2). Further bromination of the polymer (beyond 15%) results in such a dramatic decrease of the polymer diffusion that the intercalation process is too slow to be measured experimentally, even for the highest annealing temperatures we used.[41]

C. Molecular Weight Dependence. One of the most important issues in the diffusion of polymers is the dependence of the diffusion coefficient on the degree of polymerization. The D_{eff} at 170 °C is shown in Figure 5 as a function of the polymer M_w and summarized in Table 3. In these experiments polymer lengths (N) spanning a range between 2 and 52 entanglement lengths (M_w between 35 000 and 900 000) were used, and D_{eff} scales as

$$D_{eff} \propto N^{-1.09 \pm 0.05} \tag{2}$$

In the same figure the tracer diffusion coefficient of polystyrene at 170 °C is also plotted[42] according to the work of Green et al.[24,25] Following the reptation model
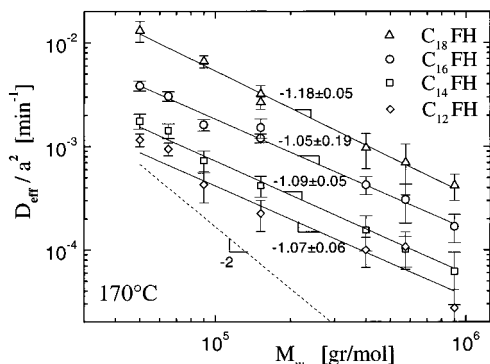
Figure 5. Molecular weight dependence of $D_{eff}/a^2 \equiv 1/\tau_{diff}$ on the polymer M_w (50 000–900 000 gr/mol) in 20 Å slit pores with four different surfaces (C12FH, C14FH, C16FH, and C18FH) at 170 °C. The slopes are from the best fits to the experimental data. The bulk self-diffusion coefficient/($a = 5$ μm)^2 at the same temperature is also shown as a dashed line, from ref 24.

in the bulk this tracer diffusion coefficient[42] follows a scaling $D_{self} \propto N^{-2}$.

D. Discussion. Before we discuss our results, we outline the three main experimental observations to be explained:

1. The filling of the silicate galleries with polystyrene occurs on a time scale ($\sim D_{eff}^{-1}$) that is faster than would be the case if the self-diffusion of polystyrene in the bulk melt governed the intercalation.

2. D_{eff} decreases approximately as N^{-1}, where N is the degree of polymerization of the polymer.

3. Increasing the interaction with the gallery walls decreases D_{eff}; increased interactions can be promoted either by adding strongly interacting PSBr units along the polymer or by decreasing the surfactant length, thus exposing more silicate surface to the polymer.

It should be understood at the outset that our D_{eff} is different from conventional polymer self-diffusion or tracer diffusion coefficients. In self-diffusion or tracer diffusion, the driving force for diffusion is the translation entropy of the polymer (i.e., $k_B T$ per polymer chain). While D_{eff} bears a superficial resemblance to an interdiffusion or mutual diffusion coefficient, where the interdiffusion of a mobile and an immobile species under a mutual enthalpic attraction is involved, the polymer chain conformations are quite different from what they would be in melt of two miscible polymers whose attractive interactions can be characterized by a negative Flory parameter χ. Perhaps the best analogue to our diffusional case is the spreading of ultrathin polymer films over an inorganic substrate that is wet by this film. The spreading of such a precursor film from a small droplet is characterized by a radius that grows as $(D_{eff}\, t)^{1/2}$ where the D_{eff} is also referred to as the diffusion coefficient of the precursor.[43] In that case, unlike ours, the polymer film, which is typically 0.5–1 nm thick, is in contact with only one surface, but the film spreads with a constant thickness that is comparable to the gallery dimensions of our intercalated silicates. In our discussion we follow the treatment of Valignat et al. in order to develop a qualitative understanding of the three major findings listed above.

Valignat et al. write an expression for their D_{eff} as

$$D_{eff} \simeq \frac{\Delta G_w}{\zeta} = \frac{G_{ll} - G_{ls}}{\zeta} \qquad (3)$$

where G_{ll} and G_{ls} are the free energies of polymer

molecules in the bulk of the droplet and in the precursor film at the solid interface, and ζ is the friction coefficient for polymer motion on the solid substrate. In our case, ΔG_w is the difference in free energy between the polymer in the polymer melt—outside the silicate gallery—and the polymer in the gallery. While the various terms that contribute to ΔG_{ls} in our case are potentially complicated, it seems clear, given the small width of the gallery and the great length of the polymer, that $\Delta G_w \propto N\Delta g_w$ where Δg_w is the free energy difference per mer unit, just as in the case considered by Valignat et al.

Thus, to give D_{eff} with a N^{-1} dependence in agreement with what we measure experimentally, the friction coefficient would have to depend on N as $\zeta \propto N^2$, which at first glance seems at odds with the usual assumption of a friction coefficient that varies as the product of the number of mers and a monomer friction coefficient ζ_0, i.e., with $\zeta \propto \zeta_0 N$. Such an assumption which is perhaps appropriate for very weak interactions between the gallery walls and the polymer would result in D_{eff} that is independent of N.

Valignat et al., in fact, observe just such an N-independent D_{eff} for spreading of poly(dimethylsiloxane) (PDMS) over oxide-covered silicon substrates, at very high relative humidity (RH $\simeq$ 98%). They attribute this molecular-weight-independent D_{eff} to masking of silanol groups, which can strongly hydrogen bond to PDMS at low RH, by water molecules at high RH. At lower RHs, however, they observe a stronger N dependence: $D_{eff} \propto N^{-0.6}$ (at RH = 80%), $D_{eff} \propto N^{-1}$ (at RH 40%), and even $D_{eff} \propto N^{-1.7}$ (at RH < 20%).[44] Valignat et al. attribute their $D_{eff} \propto N^{-1}$ (at RH = 40%) to a friction coefficient $\zeta \propto N^2$ (in fact to account for $D_{eff} \propto N^{-(a-1)}$ and $\zeta \propto N^a$ for the friction coefficient, a must vary continuously from $a = 1$ at high RH to $a = 2.7$ at low RH). They explain their results by supposing that silanol groups are not densely packed on the chemically heterogeneous oxidized silicon surfaces and form strong trapping sites for PDMS mer units. Only a small fraction of PDMS molecules that are not strongly bound to a number of such sites are free to move at any given time, but these must reptate through the already strongly adsorbed chains. Increasing RH decreases the number of such strong binding silanol sites until nearly all polymers are unbound and free to move along the surface.

We believe that a similar mechanism of that observed in the wetting experiments also accounts for our results. The walls of the silicate galleries are certainly heterogeneous, and it may be anticipated that those regions of the walls which are uncovered by surfactant tails bind strongly to PS and even more strongly to PSBr units. Molecular dynamics simulations of polymer motion in the galleries reveal the existence of very long-lived polymer "bridges", structures in which single polymer molecules are adsorbed strongly to both walls of the gallery.[19] These bridges can be expected to act as obstacles to the diffusion of unbound polymer, much as the long chains surrounding a test chain in an entangled polymer melt act to constrain its lateral motion. As mentioned by Lee et al., the number of such bridges as well as their dynamical properties is expected to depend on chain length.[19] The stronger than linear dependence of the effective wall friction coefficient ζ on chain length N we observe thus seems reasonable.

The fact that D_{eff} is larger than the self-diffusion coefficient of PS can be easily rationalized on the basis of the model of Valignat et al. if $\Delta G_w \gg 1 k_B T$, an

Table 3. Values of $1/\tau_{\text{diff}} = D_{\text{eff}}/a^2$ (min^{-1}) for a Series of M_w of PS Intercalating in C18-, C16-, C14-, and C12-FH at 170 °C[a]

M_w	$D_{\text{eff}}/a^2 \equiv 1/\tau_{\text{diff}}$ (min^{-1}) at 170 °C			
	PS in C$_{12}$FH	PS in C$_{14}$FH	PS in C$_{16}$FH	PS in C$_{18}$FH
50 000	$(1.16 \pm 0.16) \times 10^{-3}$	$(1.76 \pm 0.29) \times 10^{-3}$	$(3.84 \pm 0.41) \times 10^{-3}$	$(13.10 \pm 2.96) \times 10^{-3}$
65 000	$(0.95 \pm 0.13) \times 10^{-3}$	$(1.43 \pm 0.28) \times 10^{-3}$	$(3.05 \pm 0.32) \times 10^{-3}$	
90 000	$(0.43 \pm 0.15) \times 10^{-3}$	$(0.73 \pm 0.18) \times 10^{-3}$	$(1.62 \pm 0.21) \times 10^{-3}$	$(6.61 \pm 0.88) \times 10^{-3}$
152 000	$(0.23 \pm 0.08) \times 10^{-3}$	$(0.42 \pm 0.10) \times 10^{-3}$	$(1.20 \pm 0.12) \times 10^{-3}$	$(3.20 \pm 0.64) \times 10^{-3}$
400 000	$(0.10 \pm 0.03) \times 10^{-3}$	$(0.16 \pm 0.06) \times 10^{-3}$	$(0.43 \pm 0.08) \times 10^{-3}$	$(0.97 \pm 0.36) \times 10^{-3}$
575 000	$(0.11 \pm 0.04) \times 10^{-3}$	$(0.10 \pm 0.04) \times 10^{-3}$	$(0.31 \pm 0.13) \times 10^{-3}$	$(0.70 \pm 0.36) \times 10^{-3}$
900 000	$(0.03 \pm 0.01) \times 10^{-3}$	$(0.06 \pm 0.03) \times 10^{-3}$	$(0.17 \pm 0.05) \times 10^{-3}$	$(0.42 \pm 0.12) \times 10^{-3}$

[a] All 28 samples were annealed simultaneously in the same vacuum oven and for the same times to ensure that the annealing conditions are identical for all samples.
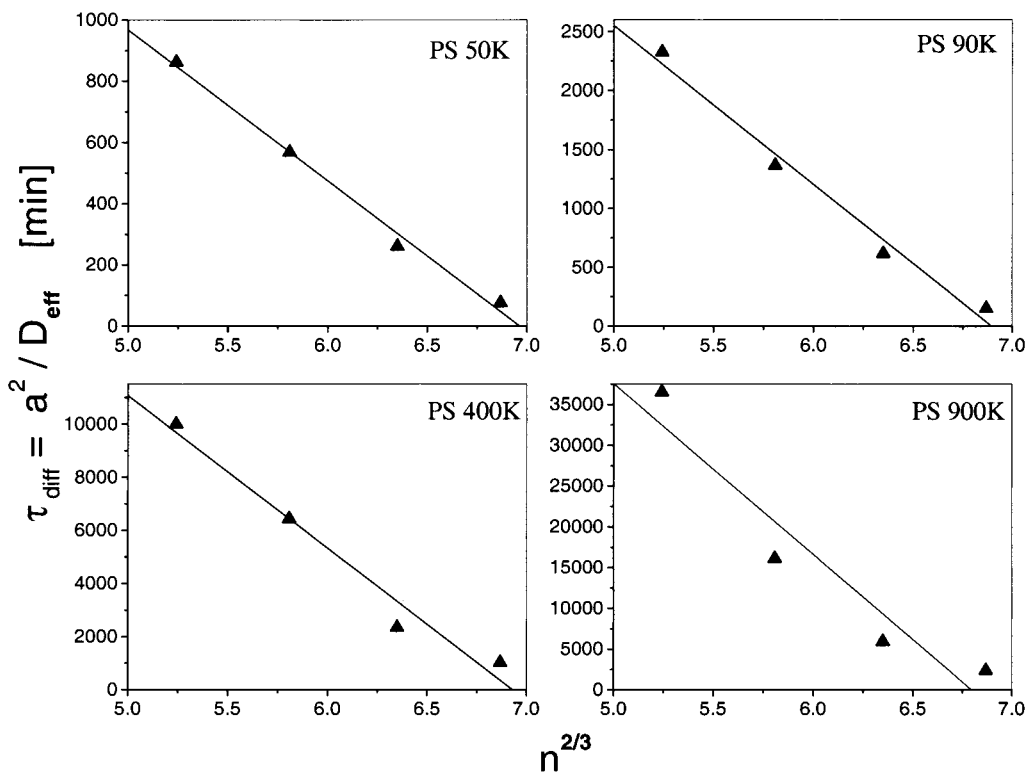
Figure 6. Same data as in Figure 3 but now plotted as $\tau_{\text{diff}} \equiv a^2/D_{\text{eff}}$ versus the surfactant length to the $^2/_3$ power ($n^{2/3}$). Four of the 16 sets measured are shown. The lines are the mean-square fits to the experimental points. The slope S and the intercept I of those lines give values of $\beta = -S/I = 0.14, 0.15, 0.14,$ and 0.15 (± 0.01) with ascending molecular weight.

inequality that would seem certain to be valid even for very moderate polymer/silicate attractions, given the long chains considered here. At the same time, given the results of Valignat et al. on the effects of RH on D_{eff}, it seems clear that an increase in the density (ρ) and strength (ϵ) of strong polymer–wall binding sites will eventually have a much stronger effect on ζ than on ΔG_w, leading to a decrease in D_{eff} with ρ and ϵ. Just such a decrease in D_{eff} with the strength of the polymer–wall affinity is also observed in the results of the simulations of Lee et al.,[19] even though the magnitude of D_{eff} was larger than the self-diffusion coefficient. Our results for D_{eff} of the PSBr$_x$ copolymers show exactly this trend, i.e., as the fraction of PSBr units—units that interact strongly with the silicate wall—increases, D_{eff} decreases.

Similarly, one would expect the density of polymer–wall interaction sites (ρ) to decrease with surfactant chain length n, since the end-grafted surfactants partly cover the surface and thus effectively reduce the interactions with the intercalating polymer (Figure 1c). Configurational biased Monte Carlo simulations[47] show that $\rho \sim 1 - \beta n^{2/3}$ for the same regime of surfactant

lengths investigated herein. Figure 6 shows the same experimental points as those in Figure 3 but now as $1/D_{\text{eff}}$ versus $n^{2/3}$, allowing us to conclude that D_{eff} depends on ρ roughly as $D_{\text{eff}} \sim \rho^{-1}$. Furthermore, beyond the CBMC finding that the density of polystyrene/surface contacts is given by a relation $\rho = 1 - \beta n^{2/3}$ (a dependence that is also anticipated by simple geometric arguments[48]), the value of the parameter β can also be calculated, since it depends only on known constants of the system, like the surfactant grafting density, the volumes of the $-CH_2-$, styrene monomer, and $-NH_3^+$, and the gallery height. For our organofluorohectorites we get $\beta \simeq 0.14$.[47] This value is in very good quantitative agreement with the linear fits from $1/D_{\text{eff}}$ versus $n^{2/3}$ for all 16 measured sets of four surfactants, for various polymer molecular weights and various temperatures (e.g., Figure 6).

Both the dependence of D_{eff} on the surfactant length n and the relative increase of the magnitude of D_{eff} between the C12FH and the C18FH systems suggest that the change of the polymer total friction coefficient—rather than the dilution of the polymer by the surfactant

(Appendix A and also Figure 7)—determines the diffusion of PS near these surfactant bearing surfaces. Furthermore, both the neutron scattering findings and the strong dependence of D_{eff} on the surfactant—that exists *only* end-grafted on the silicate walls—clearly indicate that we are probing the confined polymer motion inside the silicate galleries and not any mass transport process that the bulk polymer undergoes while approaching the silicates.

Finally, while it might be tempting to draw parallels between our data and recent simulations and experiments on two-dimensional diffusion of dilute chains,[49−52] there is an important fundamental difference: namely in those cases the polymer motion is driven by translational entropy of the dilute chains, i.e., the ΔG driving force in eq 3 is $k_B T$, and thus independent of chain length. In those cases, the experiments show that the effective polymer friction coefficient ζ scales as N (for DNA on a cationic lipid membrane[51]) and as $N^{3/2}$ for poly(ethylene oxide) "pancakes" on organically modified silica.[52] The arguments advanced in the latter case to account for the stronger than linear dependence of ζ on N are similar to the ones suggested herein.

IV. Conclusions

From concurrent SANS and IANS studies of the kinetics of intercalation of polystyrene in organically modified silicates, it is shown that the silicate gallery expansion (measured through IANS or XRD) reflects directly the motion inside the 2 nm slit pore of the polymer chains (the conformation of which is simultaneously followed by SANS). Thus, XRD studies allow for the study of polymer mobility in extreme 2 nm confinements by monitoring the intercalation kinetics of model polystyrene polymers in inorganic layered hosts (2:1 phyllosilicates).

For the same polymer and the same annealing temperature, the experimentally measured effective diffusion coefficient depends strongly on the surfactant used, i.e., the nature of the surfaces inside the interlayer galleries. Because the surfactant can only affect the mobility of the physisorbed polymers, one concludes that the motion of the polymers in the interlayer is the process that dictates the intercalation kinetics, and thus the measured D_{eff} traces the diffusion coefficient of the confined polymer *inside* the 2 nm slit pore.

For several different polymer molecular weights and annealing temperatures we observe that D_{eff} increases markedly with longer surfactant lengths and much more than is expected just from the enhancement of polymer mobility resulting from the polymer dilution by small hydrocarbon oligomers (Appendix A). Longer surfactants result in less silicate surface area exposed to the polymer, thus effectively reducing the density of attractive sites. D_{eff} scales inversely with this site density. Moreover, introducing along the PS chain random Br groups that interact strongly with the silicate surface, thus increasing the strength of the attractive sites, results in a strong decrease of D_{eff}. Thus, increasing either the density or the strength of these attractive sites leads to much slower intercalation kinetics. This is the case despite the fact that an increase in site density or strength must also increase the driving force (ΔG_w) for intercalation; evidently such increases depress the friction coefficient ζ much more strongly.

Finally, the diffusion coefficient D_{eff} scales with N^{-1}, for polystyrenes with M/M_e ranging from 2 to 52 and

for four different surfactant−silicate galleries. Although these same polymers would show a polymer self-diffusion that scales with N^{-2} in the bulk,[24,53] they show diffusion coefficients that scale with N^{-1} when confined to the ultranarrow slit pores with attractive surface sites investigated here. A qualitative explanation of the diffusion behavior under these confined conditions is given based on an analogy to the spreading of 1 nm polymer precursor films on solid surfaces[43] and insight from molecular simulations.[19,47]

The measurements in this present study touch upon the more general problem of polymer transport in nanometer confinements. We hope that these measurements will motivate theoretical approaches that will go beyond the preliminary/qualitative arguments provided herein.

Appendix A

On the basis of the reptation theory[53,54] and on experimental observations,[55,56] one can estimate how the diffusion coefficient of long polymers in dilution[58] depends on the polymer concentration (ϕ). The dependence of the diffusion coefficient $D(\phi)$ compared to the tracer diffusion coefficient of the undiluted polymer in the same geometry (D_{eff}) is given by

$$\frac{D(\phi)}{D} \propto \frac{\zeta_0}{\zeta_0(\phi)} \frac{1}{\phi^d} \qquad (4)$$

where ζ_0 is the monomeric friction coefficients of the confined polymer in absence of any small molecules, $\zeta_0(\phi)$ is the monomeric friction coefficient under dilution by the aliphatic surfactants, and ϕ is the polymer volume fraction. The ratio $\zeta_0/\zeta_0(\phi)$ reflects primarily how the glass transition, and thus the local dynamics, change by dilution. The ϕ^d factor accounts for the reduction in both the concentration of chains and the number of entanglements per chain, and the value of d is close to 1 (Tead and Kramer[55] report $d = 1$ and Graessley[56] $d = 1.4$). Since the monomeric friction coefficients are proportional to the respective zero shear rate viscosities (η_0), their ratio can be written in terms of the WLF shift factors[57] ($\eta_0 \propto \alpha_T(T - T_g)$). Assuming the strongest dependence on the polymer concentration (i.e., $1/\phi^{1.4}$), eq 4 can be rewritten as

$$\frac{D(\phi)}{D_{melt}} \propto \frac{\alpha_T(T - T_g)}{\alpha_T(T - T_g(\phi))} \frac{1}{\phi^{1.4}} \qquad (5)$$

One can approximate the glass transition of the diluted
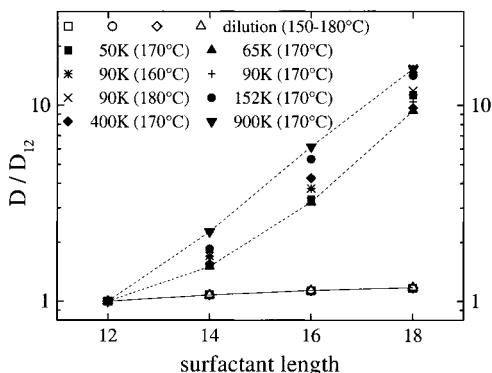
Figure 7. Diffusion coefficients versus the surfactant length normalized by the D_{eff} for C12FH. Solid symbols experimental points, open symbols D_{eff} as predicted by eq 5 if the polymer dilution by the surfactant molecules was the only effect changing the polymer mobility (data tabulated in Table 4). The dashed lines are the envelopes of the experimental points and the solid lines of the predictions by eq 5.

Table 4. Effect of Increased Surfactant Concentration on the Diffusion Coefficients for Several Temperatures[a]

	PS M_w	PS/ C$_{12}$FH	PS/ C$_{14}$FH	PS/ C$_{16}$FH	PS/ C$_{18}$FH
ϕ		0.79	0.75	0.72	0.68
w_1 (wt % polymer)		0.68	0.65	0.63	0.62
w_2 (wt % surfactant)		0.32	0.35	0.37	0.38
from polymer dilution arguments					
D/D$_{12}$ (150 °C)		1	1.080	1.133	1.164
D/D$_{12}$ (160 °C)		1	1.079	1.134	1.168
D/D$_{12}$ (170 °C)		1	1.078	1.134	1.171
D/D$_{12}$ (180 °C)		1	1.077	1.135	1.175
experimental results					
D/D$_{12}$ (160 °C)	90K	1	2.26	4.25	10.42
D/D$_{12}$ (170 °C)	90K	1	1.70	3.77	15.37
D/D$_{12}$ (180 °C)	90K	1	1.63	3.23	11.84
D/D$_{12}$ (170 °C)	50K	1	1.52	3.31	11.26
D/D$_{12}$ (170 °C)	65K	1	1.51	3.21	9.38
D/D$_{12}$ (170 °C)	152K	1	1.85	5.32	14.18
D/D$_{12}$ (170 °C)	400K	1	1.55	4.26	9.70
D/D$_{12}$ (170 °C)	900K	1	2.27	6.17	15.34

[a] The weight fractions were measured by TGA in samples intercalated *at exchange capacity*. The calculation of the dilution effect $D(\phi)$ is based on eqs 4−6 and are normalized by the diffusion coefficient for PS in C12FH at each annealing temperature. Some of the experimental results—for various M_w's and temperatures—are also shown for comparison.

polymers from the inverse rule of mixtures and the α_T from

$$\log(\alpha_T) = \frac{-c_1(T - T_g)}{c_2 + T - T_g} \quad \text{and} \quad \frac{1}{T_g(\phi)} = \frac{w_1}{T_g^1} + \frac{w_2}{T_g^2} \quad (6)$$

We can use $c_1 = 13.7$ and $c_2 = 50$ for PS[57] and T_g as the reference temperature. The weight fractions of the polymer (w_1) and the surfactant (w_2) were directly measured from thermal gravimetric analysis (TGA) of PS/C$_{12-18}$FH samples intercalated *at exchange capacity*, i.e., where there exists no free—unintercalated—polymer.[59]

Assuming the strongest dependence on concentration (eq 5) and subsequently normalizing for each temperature all diffusion coefficients with the respective $D(\phi)$ for the C12FH systems, we can estimate the *upper limit* of the effect that the increasing diluter concentration has on the diffusion coefficient (tabulated in Table 4). These results are compared with the experimentally

measured values of D_{eff} in Figure 7. Thus, D_{eff} is expected to increase by about 20% from C12FH to C18FH due to polymer dilution, whereas experimentally a 10-fold increase is observed.

Obviously, although the existence of the diluter molecules does increase the polymer mobilities substantially from their bulk values, it does not account for the 10-fold increases in D_{eff} with surfactant length found in this study (Table 4). The effect that underlies our enhanced mobilities is the reduction in friction caused by an increased coverage of the surface by the organic surfactant, as discussed in section III.B (Figure 6).

Appendix B

The functionalization of a polymer may cause a change in its tracer diffusion coefficient, especially in the cases where this functionalization introduces additional constraints on individual chain motion.[60] However, bromination is expected not to change the polystyrene self-diffusion,[61] especially for the level of bromination used in this study ($\leq 15\%$). To verify this assumption, we carried out melt state rheology studies that can directly compare the relaxation behavior—and through the shift factors a_T also the diffusion—of the neat polystyrene and its brominated derivative.

The tracer diffusion difference between the styrene and its brominated derivative is expected to be the largest for larger molecular weights and higher functionalization levels;[60] thus, we selected the highest M_w polystyrene that we brominated ($M_w = 575\,000$, labeled PS575) and its 9 mol % brominated derivative (labeled PS575-Br9). The melt state rheology of this pair was studied by the application of dynamic oscillatory shear using a parallel plate ARES rheometer. The samples were prepared by vacuum molding at 160 °C into 25 mm diameter disks and kept under vacuum at ambient temperature until just prior to use. The melt rheology was performed under a nitrogen atmosphere to prevent thermal oxidation or degradation and measurements were repeated at several strains and temperatures to ensure the viscoelastic data were linear. The master curves obtained by superpositioning of data taken at different temperatures to a reference temperature of 160 °C are shown in Figure 8. The horizontal shift factors, a_T, used to produce these master curves are shown in Figure 9. The horizontal shift factors are quite similar, although the shift factors for the bromopolystyrene are marginally faster than the polystyrene. In addition, small vertical shift factors ($0.98 < b_T < 1.03$) were also used and are consistent with the effect of temperature on the density. In addition, a direct comparison of the viscoelastic spectrum confirms that the terminal relaxation time (as measured by the crossover of G' and G'') is increased for the brominated sample and increases by a factor of less than 3 at 160 °C. However, the overall shape of the viscoelastic spectrum is very similar for the pure polystyrene and the brominated polystyrene and consistent with that of a monodispersed homopolymer.

This 3-fold increase of the terminal relaxation time suggests a similar decrease in the polymer tracer diffusion with bromination, since a_T and T_g remain the same and R_g is not expected to change more than 5% for the 9% brominated polystyrene.[40] This moderate decrease in bulk diffusion cannot account for the very strong decrease in D_{eff} in the C12FH samples (about 56 times lower for 8% PBrS compared to the D_{eff} of the
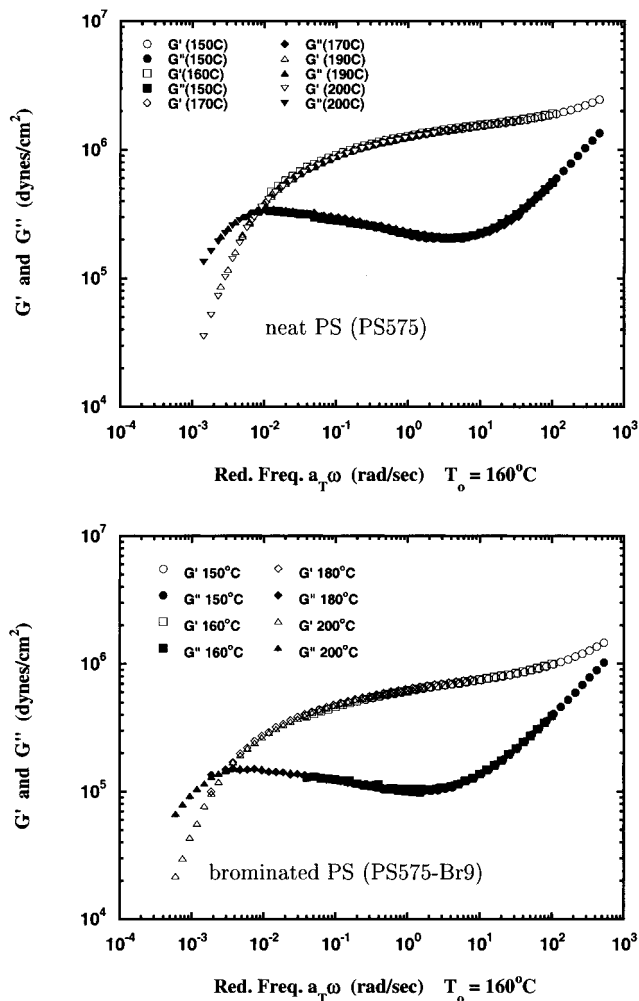
Figure 8. Melt state rheology of PS M_w = 575 000 (PS575) and its 9.2 mol % brominated derivative (PS575-Br9). Dynamic oscillatory shear in a parallel plate geometry was employed, and measurements were repeated at several strains and temperatures to ensure the viscoelastic data were linear. The master curves were obtained by superpositioning of data taken at different temperatures to a reference temperature of 160 °C.
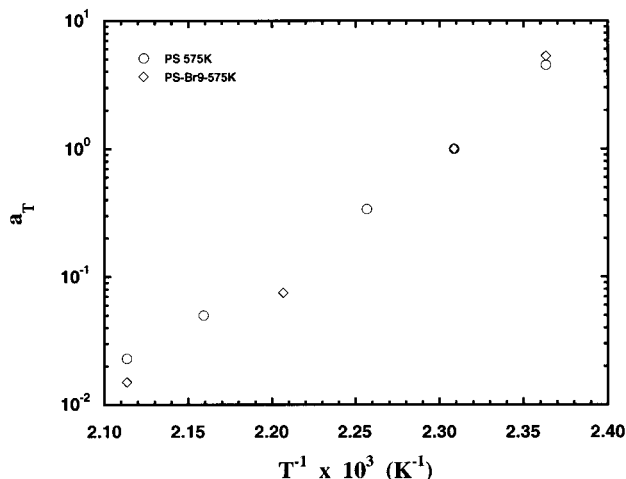
Figure 9. Horizontal shift factors, a_T, used to produce the master curves of Figure 8.

unmodified PS; Table 2). Moreover, for longer sur-factants—less exposed surface to the brominated polymer—there is hardly any difference in the D_{eff} of neat and 9% brominated PS (e.g., C16FH systems in

Table 2), as the role of the bromine energetics diminishes near such organically covered surfaces. Thus, we can conclude that the change of the polymer−surface energy of adsorption with bromine—rather than the moderate change of the polymer tracer diffusion coefficient—is the origin of the strong D_{eff} reduction in our 2 nm confines.

References and Notes

(1) Manias, E.; Subbotin, A.; Hadziioannou, G.; ten Brinke, G. *Mol. Phys.* **1995**, *85*, 1017.
(2) Bitsanis, I.; Pan, C. *J. Chem. Phys.* **1993**, *99*, 5520.
(3) Horn, R. G.; Israelachvili, J. N. *Macromolecules* **1988**, *21*, 2836.
(4) Montfort, J. P.; Hadziioannou, G. *J. Chem. Phys.* **1988**, *88*, 7187.
(5) Horn, R. G.; Hirz, S. J.; Hadziioannou, G.; Frank, C. W.; Catala, J. M. *J. Chem. Phys.* **1989**, *90*, 6767.
(6) van Alsten, J.; Granick, S. *Macromolecules* **1990**, *23*, 4856.
(7) Homola, A. M.; Nguyen, H. V.; Hadziioannou, G. *J. Chem. Phys.* **1991**, *94* 2346.
(8) Klein, J.; Perahia, D.; Warburg, S. *Nature* **1991**, *352*, 143.
(9) Hirz, S. J.; Homola, A. M.; Hadziioannou, G.; Frank, C. W. *Langmuir* **1992**, *8*, 328.
(10) Granick, S.; Hu, H. W. *Langmuir* **1994**, *10*, 3857, 3867.
(11) Anastasiadis, S. H.; Karatasos, K.; Vlachos, G.; Manias, E.; Giannelis, E. P. *Phys. Rev. Lett.* **2000**, *84*, 915.
(12) Giannelis, E. P.; Krishnamoorti, R.; Manias, E. *Adv. Polym. Sci.* **1998**, *138*, 107.
(13) Krishnamoorti, R.; Vaia, R. A.; Giannelis, E. P. *Chem. Mater.* **1996**, *8*, 1728.
(14) Giannelis, E. P. *Adv. Mater.* **1996**, *8*, 29.
(15) Vaia, R. A.; Jandt, K. D.; Kramer, E. J.; Giannelis, E. P. *Macromolecules* **1995**, *28*, 8080.
(16) Doi, M. *Introduction to Polymer Physics*; Oxford University Press: New York, 1996.
(17) Rowlinson, J. S.; Widom, B. *Molecular Theory of Capillarity*; Oxford University Press: New York, 1982.
(18) Cracknell, R. F.; Nicholson, D.; Quirke, N. *Phys. Rev. Lett.* **1995**, *74*, 2463.
(19) Lee, J. Y.; Baljon, A. R. C.; Loring, R.; Panagiotopoulos, A. Z. *J. Chem. Phys.* **1998**, *109*, 10321; **1999**, *111*, 9754.
(20) Barrer, R. M.; Craven, R. J. B. *J. Chem. Soc., Faraday Trans.* **1992**, *88*, 645. Breen, C.; Deane, T.; Flynn, J. J.; Reynolds, D. *Clays Clay Mineral.* **1987**, *17*, 198. Kärger, J.; Ruthven, D. *Diffusion in Zeolites*; J. Wiley & Sons: New York, 1992.
(21) The silicate crystalline layer thickness is 9.7 Å; thus, a *d* spacing of 30 Å corresponds to approximately 20 Å of confined organic film.
(22) Demeter, J.; Giannelis, E. P. Kinetics of end-funcionalized polystyrene in organically modified silicates. Manuscript in preparation.
(23) Vaia, R. A.; Jandt, K. D.; Kramer, E. J.; Giannelis, E. P. *Chem. Mater.* **1996**, *8*, 2628.
(24) Green, P. F.; Palmstrom, C. J.; Mayer, J. W.; Kramer, E. J. *Macromolecules* **1985**, *18*, 501.
(25) Green, P. F.; Kramer, E. J. *J. Mater. Res.* **1986**, *1*, 202.
(26) Zheng, X.; Sauer, B. B.; Van Alsten, J. G.; Schwarz, S. A.; Rafailovich, M. H.; Sokolov, J.; Rubinstein, M. *Phys. Rev. Lett.* **1995**, *74*, 407; **1997**, *79*, 241.
(27) Frank, B.; Gast, A. P.; Russell, T. P.; Brown, H. R.; Hawker, C. *Macromolecules* **1996**, *29*, 6531.
(28) Russell, T. P. Private communication.
(29) Composto, R. J.; Mayer, J. W.; Kramer, E. J. *Phys. Rev. Lett.* **1986**, *57*, 1312.
(30) Subbotin, A.; Semenov, A. N.; Manias, E.; Hadziioannou, G.; ten Brinke, G. *Macromolecules* **1995**, *28*, 1511.
(31) Krishnamoorti, R. Manuscript in preparation.
(32) Manias, E.; Kuppa, V.; Yang, D.-K.; Zax, D. B. *Colloids Surf. A*, in press.
(33) Mattice, W. L.; Suter, U. W. *Conformational Theory of Large Molecules: The Rotational Isomeric State Model in Macromolecular Systems*; Wiley: New York, 1994. Robyr, P.; Gan, Z.; Suter, U. W. *Macromolecules* **1998**, *31*, 8918.
(34) For example: Sun, H.; et al. COMPASS force field (MSI). Berendsen, H.; et al. GROMACS (University of Groningen). Cuthbert, T. R.; Wagner, N. J.; Paulaitis, M. E. *Macromolecules* **1997**, *30*, 3058. Roe, R.-J; Mondello, M.; Furuya, H.; Yang, H.-J. *Macromolecules* **1995**, *28*, 2807. Roe, R.-J. *J. Noncryst. Solids* **1998**, *235*, 308.
(35) Muller-Plathe, F. *Macromolecules* **1996**, *29*, 4782.

(36) Hackett, E.; Manias, E.; Giannelis, E. P. *J. Chem. Phys.* **1998**, *108,* 7410.

(37) Silberzan, P.; Leger, L.; Ausserre, D.; Benattar, J. J. *Langmuir* **1991**, *7,* 1647. Migler, K. B.; Massey, G.; Hervet, H.; Leger, L. *J. Phys.: Condens. Matter* **1994**, *6,* A301.

(38) Nakamura, M.; Koshino, K.; Matsuo, J. *Jpn. J. Appl. Phys.* **1992**, *31,* 1999; **1993**, *32,* 3063. Flaum, H. C.; Sullivan, D. J.; Kummel, A. C. *J. Phys. Chem.* **1994**, *98,* 1719.

(39) Kambour, R. P.; Shultz, A. R. *Macromolecules* **1986**, *19,* 2679.

(40) Strobl, G. R.; Bendler, J. T.; Kambour, R. P.; Shultz, A. R. *Macromolecules* **1986**, *19,* 2683. Malhotra, S. L.; Lessard, P.; Blanchard, L. P. *J. Macromol. Sci., Chem.* **1981**, *A15,* 1577.

(41) From the initial stages of intercalation of a 25% brominated polystyrene $M_w = 152K$ in C12FH, we estimate a decrease of more then 1800 times in D_{eff}, compared to the D_{eff} of neat PS confined into the same surfaces.

(42) The tracer diffusion experimental data are translated into D_{eff} values by assuming a lateral silicate size of 5 μm.

(43) Valignat, M. P.; Oshanin, G.; Villette, S.; Cazabat, A. M.; Morceau, M. *Phys. Rev. Lett.* **1998**, *80,* 5377.

(44) Heslot, F.; Cazabat, A. M.; Levinson, P.; Frazee, N. *Phys. Rev. Lett.* **1990**, *65,* 599.

(45) Vaia, R. A.; Giannelis, E. P. *Macromolecules* **1997**, *30,* 8000.

(46) Balazs, A. C.; Singh, C.; Zhulina, E. *Macromolecules* **1998**, *31* 8370.

(47) Hackett, E.; Giannelis, E. P.; Manias, E. *J. Chem. Phys.,* submitted.

(48) This $n^{2/3}$ dependence is something that can be easily anticipated also along the lines of the following simple argument: Due to symmetry parallel to the confining surfaces, the average shape of the surfactant would be symmetric by rotation (i.e., the solid created by rotating the density profile of Figure 1d around the *z*-axis and is similar to three overlapping spheres on top of each other). With increasing n the surfactant volume would increase as $\sim n$, so its radius at the surface would increase as $\sim n^{1/3}$ and thus the surface area that it would cover would scale like $\sim n^{2/3}$.

(49) Carmesin, I.; Kremer, K. *Macromolecules* **1988**, *21,* 2819.

(50) Milchev, A.; Binder, K. *Macromolecules* **1996**, *29,* 343.

(51) Maier, B.; Rädler, J. O. *Phys. Rev. Lett.* **1999**, *82,* 1911.

(52) Sukhishvili, S. A.; Chen, Y.; Muller, J. D.; Gratton, E.; Schweizer, K. S.; Granick, S. *Nature* **2000**, *406,* 146.

(53) Doi, M.; Edwards, S. F. *The Theory of Polymer Dynamics*; Oxford University Press: New York, 1986.

(54) Graessley, W. W. *Adv. Polym. Sci.* **1983**, *47,* 76.

(55) Tead, S. F.; Kramer, E. J. *Macromolecules* **1988**, *21,* 1513.

(56) Graessley, W. W. *Physical Properties of Polymers,* 2nd ed.; American Chemical Society: Washington, DC, 1993; Chapter 3. Berry, G. C.; Fox, T. G. *Adv. Polym. Sci.* **1968**, *5,* 261. Pearson, D. S. *Rubber Chem. Technol.* **1987**, *60,* 439.

(57) Ferry, J. D. *Viscoelastic Properties of Polymers*; J. Wiley & Sons: New York, 1980.

(58) The polymers could be diluted by either solvents, or plasticizing agents, or even polymer chains of smaller molecular weight than the polymer in discussion.[55,57]

(59) Zax, D. B.; Yang, D.-K.; Santos, R. A.; Hegemann, H.; Giannelis, E. P.; Manias, E. *J. Chem. Phys.* **2000**, *112,* 2945.

(60) Colby, R. H.; Zheng, X.; Rafailovich, M. H.; Peiffer, D. G.; Schwarz, S. A.; Strzhemechny, Y.; Nguyen, D. *Phys. Rev. Lett.* **1998**, *81,* 3876.

(61) Genzer, J. Ph.D. Thesis, U Penn, 1996.